Bio-engineering of neuromesodermal progenitors

Jorge Miguel Faustino Martins[1], MSc in Biomedical Engineering, 73615
MEBiom, jorge.martins@tecnico.ulisboa.pt
Supervisors: Prof. Maria Margarida Fonseca Rodrigues Diogo[1] and Prof. Domingos Manuel Pinto Henrique[2]

[1] Instituto Superior Técnico, (IST), Universidade de Lisboa, Lisbon, Portugal

[2] Instituto de Medicina Molecular, (IMM), Faculdade de Medicina da Universidade de Lisboa, Lisbon, Portugal

November, 2016

Abstract: Neuromesodermal progenitors (NMPs) are a cell population that has been pointed as responsible for generating both posterior neural precursors and mesoderm derivatives that will develop into the spinal cord. These progenitors function during embryonic gastrulation, when epiblast cells undergo differentiation to establish three germ layers (endoderm, mesoderm, and ectoderm) that will give rise to all tissues in the embryo. NMPs have been studied *in vitro,* using a protocol for three-dimensional (3D) generation of cell aggregates, entitled gastruloids, through self-organization in presence of Wnt pathway agonists that activate polarized 3D elongation. However, this method has limitations, concerning efficiency and reproducibility of the process. In this work, I aimed at developing more robust methods to generate and propagate NMPs in culture, starting from mouse embryonic stem cells (mESCs). To achieve this aim, I employed a mechanical scaffold during *in vitro* gastruloid development, using poly(lactic-co-glycolic acid) (PLGA) fibers. To monitor the process, I used morphological approaches in which aggregates were counted and measured, while also doing fluorescence detection with Sox1::GFP cells and immunofluorescence with relevant molecular markers for NMPs. Results show an increase in successful gastruloid formation and elongation when PLGA was used, while also exhibiting a patterned cell growth with less variability, thus representing a more robust protocol than the original one where fibers were not used. Additionally, I found that neural tissue emerging in extending fiber-supported gastruloids are organized in a neural tube-like structure, showing hints of apicobasal epithelial polarity, suggesting that PLGA fibers provide adequate mechanical support for tissue organization.

Key words: Embryonic stem cells; Neuromesodermal progenitors; Spinal cord; Poly(lactic-co-glycolic acid); Gastruloid;

Introduction

Gastrulation is a process that marks embryonic development, after a spatial reorganization of the embryo following uterine implantation, when it consists of two main cell layers, proximal epiblast and distal visceral endoderm. From the epiblast, cells are recruited in a 'dropping' motion to the primitive streak, a transition zone that marks the anterior-posterior axis [1]. Cells recruited in this fashion will then give rise to mesoderm or endoderm (depending on their position), organizing themselves in an intermediate layer entitled mesendoderm [1, 2].
This process is characterized by the lengthening of the primitive streak due to an expansion of the recruitment process towards anterior regions of the embryo. The limit is then marked by a broader dampening region called the primitive node, ending the first step of gastrulation [3-5].

After this, a regression of the streak is observed, in which precursor populations will leave in its place mesodermal populations and neural plate cells, which will then fold into the neural tube, a precursor for the posterior central nervous system [6-9]. Besides these, the notochord is also formed, which is a tubular structure that serves as an important signaling center for neural development and mesoderm recruitment. The cells responsible for the generation of both neural and mesodermal posterior tissue are neuromesodermal progenitors (NMPs), which are bipotent cells originated during gastrulation and laid close to the node as the primitive streak regresses [10].
The discovery of these cells was important to hypothesize that the anterior and posterior nervous systems have different and independent origins, unlike what was previously thought with

the “Activation-Transformation” theory [11, 12]. This hypothesis stated that the anterior central nervous system (CNS) was entirely formed and then, through the action of posteriorizing signals, some populations transformed into posterior CNS.

NMPs, for their role in generating precursor spinal cord tissue, hint at the independence between anterior and posterior CNS development. These cells were isolated *in vivo* from activation of the epiblast during gastrulation at the caudal lateral epiblast (CLE) and the node-streak border (NSB) [10].

Even though they are not considered a stem cell population *per se* due to limited proliferative potential and tendency towards differentiation, they are still a dynamic progenitor population with fluctuating numbers during embryonic development that accompanies the regression of the streak and leads to neural or mesodermal tissues with different gene expression profiles [10, 13].

NMPs can also be generated *in vitro*, through differentiation of ESCs. This process requires the use of a GSK3 inhibitor to activate the Wnt pathway on three-dimensional (3D) aggregates that form spontaneously through self-organization of ESCs in suspension, when present in low attachment conditions [14]. These aggregates are known as gastruloids since they provide a 3D representation of the gastrulation process that occurs *in vivo*. Although not the only option in cell culture to generate NMPs, gastruloids are preferred to monolayer culture. This is due to the fact that the latter involves cell culture in a flat sheet and even if it is useful to study specific low-scale processes, it fails to represent events at a larger scale, since gastrulation is a 3D process.

NMPs may then be characterized through the detection of simultaneous expression of both neural (*Sox2*) and mesodermal (*Brachyury*) markers [10].

As mentioned above, even though there are still some molecular cues to be clarified during NMP generation, Wnt signaling pathway is already known to play a major role in the process.

The canonical pathway of Wnt is characterized by the constant degradation of transcriptional regulator β-catenin in the intracellular medium by a complex which GSK-3 is a part of.

The binding of Wnt proteins to membrane receptor complexes will lead to a signal transduction cascade that originates the coupling of proteins from the degradation complex to the membrane. This will promote stabilization of β-catenin and a consequent increase in its levels in the cytoplasm. This protein will then migrate towards the cell nucleus and activate transcription of Wnt target genes that lead to the development of NMPs and their commitment to precursor lineages [15-20].

In vitro, the same role is achieved by the use of a chemical inhibiting the GSK-3 complex. However, this process is associated with a high level of variability, related to the number of formed aggregates and the way they elongate based on Wnt chemical pulse.

In that sense, recent studies [21] show that the use of a poly(lactic-co-glycolic acid) (PLGA) fiber cultured together with the cells would optimize the protocol and reduce variability in a brain organoid model.

This results from the fact that the fiber comes from a stable polymer with an almost neutral (with a tendency towards hydrophobic) behavior that is already used as a biodegradable suture and, therefore, is already prepared to interact with living tissue and allows for cells to adhere.

Finally, there is also evidence that to direct stem cell differentiation towards a certain lineage, not only chemical cues are important, but also mechanical properties such as stiffness play an important role in mimicking extracellular matrix (ECM) and therefore affect tissue development upon interaction with cells [22, 23].

Therefore, this project had the aim of reducing variability associated with 3D gastruloid culture. In that sense, achieving a more robust protocol would result in less randomness related to aggregate formation and elongation, which usually happens in an uncontrolled way. To achieve this, mouse embryonic stem cells (mESCs) were cultured in the presence of PLGA fibers that provide a physical backbone for cells to agglomerate and elongate alongside. This had the objective of achieving a patterned extension of gastruloids, with resemblances to primordial tissue organization that could in the future provide further insight into the gastrulation process by mimicking it *in vitro*.

Methods

mESC culture

The mESCs used in this work were derived from the murine cell lines E14 and 46C (a Sox1::GFP line for neural development reporting). These cell lines had been frozen on 10/03/2015 in the E14 case, and on 13/02/2015 for the 46C line. Both cell lines originated from the laboratory of Professor Domingos Henrique at Instituto de Medicina Molecular, in Lisbon, and were frozen by Master’s Student Andreia Pereira. These cells were cultured in serum-containing medium GMEM, supplied with Leukemia Inhibitory Factor (LIF) (1:500, originally at 30 ng/μL). Cultures were all maintained in incubation at 37ºC under a 5% CO2 humidified atmosphere.

mESCs cell passaging

The cells were washed twice with 5 mL of Phosphate Buffered Saline (PBS) and incubated with 500 µL 0.1% Trypsin-EDTA (originally at 2.5%, GIBCO) for 2 minutes at 37ºC. Then, after observing the successful dissociation of the cells from the plate surface on the microscope, the trypsin was inactivated using 4 times the trypsin volume of GMEM and the cells were centrifuged at 1200 rpm for 4 min. After removing the supernatant, the pellet was resuspended in 1 mL GMEM and the cells were counted using trypan blue exclusion method on the microscope, using a counting chamber. Finally, the cells were seeded at a density of 30 000 cells/cm2 using GMEM+LIF in previously gelatin-coated dishes.

Aggregate formation

After two passages of mESCs in normal expansion conditions, cells were left until reaching 40-60% confluence (over-confluent cells do not form stable aggregates), washed twice with 5 mL PBS, and dissociated using 500 µL trypsin, which was inactivated with four times the trypsin volume used of GMEM, followed by centrifugation at 1200 rpm for 4 min. The supernatant was removed and the cells were resuspended in 1 mL GMEM and counted, using trypan blue as an exclusion viability marker and a counting chamber. The cells were then resuspended in 1 mL pre-warmed PBS at a density of 75 000 cells/mL (600 cells/well) and centrifuged at 1200 rpm for 4 min. The supernatant was then removed and the previous step was repeated. After washing with PBS for the second time, the pellet was resuspended in 1 mL warm N2B27 in a homogeneous suspension, followed by addition of N2B27 (Thermo Fisher) until a total of 5 mL suspension was reached. The cell suspension was then pipetted in droplets of 40 µL/well into the bottom of each well in a non-treated 'U'-bottomed 96-well plate (Cellstar) using a multichannel pipette, followed by a further 40 µL/well of N2B27 medium with PLGA fibers previously sliced and sheared. Finally, each well was filled with N2B27 up until 150 µL/well and left to incubate for 48 h at 37ºC. Following that period of time, the presence of aggregates was confirmed by observing the plates on the microscope. Then, 90 µL of the medium was removed and replaced with 90 µL fresh secondary medium CHIRON (3 µM Chi99021 (Chi) 1:1000 in N2B27, stock prepared at 3 mM in DMSO) in each well with a multichannel pipette and then left to incubate for 24 h at 37ºC. Culture medium was changed every 24 h (until a total of 120 h since the beginning of the experiment) using a multichannel pipette held at approximately 30º to remove 90 µL of medium present in culture and replace it with 90 µL of fresh N2B27 in each well.

PLGA sterilization

PLGA fibers (commercialized as Vicryl, Ethicon) were cut and sheared under the microscope using a surgical blade and stored in a P60 plate in PBS while being exposed to UV light for 15-20 min for sterilization. The microfibers were obtained by cutting a 5 cm-long portion of the original fiber, in order to obtain on average 5-10 microfibers per well. The polymeric fibers were not longer than 1 mm nor wider than 0.5 mm. They were collected from the P60 plate in a washing step with 5 mL N2B27, passing the medium several times on the plate to remove the microfibers (constant observation while performing this step was crucial due to the slightly hydrophobic nature of the biomaterial that may lead it to adhere to the plate instead of being washed away) before placing them in each well, using a plastic reservoir and a multichannel pipette.

Fluorescence microscopy

When using fluorescence microscopy for Sox1:GFP detection, 150 µL of medium were removed from each well in the 96-well plate and washed twice with 150 µL PBS, leaving a couple of minutes between washing steps to let the aggregates settle. This allows the reduction of autofluorescence associated with N2B27 and to wash away some fibers that did not support any cells and are also very autofluorescent, resulting in a heavy 'echoing effect' in the pictures when they are massively present.

Immunohistochemistry

Fixation and primary antibody incubation

The wells with aggregates selected for immunofluorescence were washed twice with 150 µL PBS, after having 150 µL N2B27 removed, with a couple of minutes between washing steps to let the aggregates settle. Then, with a cut P1000 tip, 250 µL were removed from each selected well and placed in a glass dissection well, placing all aggregates that undergo the same staining conditions on the same well. Using a glass Pasteur pipette (Sigma), the liquid was drawn from each dissection well carefully not to aspirate any aggregate nor to drain the well completely, so the aggregates would not dry. After that, the aggregates were fixed with 1 mL 4% paraformaldehyde (PFA) solution (Sigma) for 2 hours at 4ºC in an orbital shaker set to low speed. The fixating agent was then washed with

PBS three times, in 10 min steps each. The PBS was then aspirated and replaced with a 1 mL solution of PBS containing 10% FBS and 0.2% Triton X-100 (PBSFT) for three 10 min washing steps on an orbital shaker at low speed at 4ºC. The aggregates were then blocked for 1 h in 1 mL PBSFT at 4ºC on an orbital shaker set to low speed, followed by an overnight incubation step with a 500 µL solution of the primary antibody (see Table 1) diluted in PBSFT at 4ºC on an orbital shaker set to low speed. The wells need to be covered in paraffin to prevent evaporation.

Secondary antibody incubation

The primary antibody solution was aspirated the following day and washed with 1 mL PBSFT at 4ºC in the following manner: twice for 5 min, thrice for 15 min and seven times for 1 h, in an orbital shaker set to low speed. The medium needed to be chilled for these steps. Then, the final washing solution was aspirated and the aggregates were incubated overnight with the correspondent secondary antibody (see Table 2), adding also 3 µL of 4'',6-Diamino-2-Phenylindole dilactate (DAPI) nuclear staining in a 500 µL solution diluted in PBSFT at 4ºC in the dark on an orbital shaker, sealed with paraffin to avoid evaporation.

Mounting and imaging

The next day, the secondary antibody solution was aspirated and the aggregates were washed with a 1 mL solution of PBS containing 0.2% FBS and 0.2% Triton X-100 (PBT) twice for 5 min and thrice for 15 min, at room temperature (RT) on an orbital shaker protected from light. The washing solution was afterwards aspirated and the aggregates were incubated at RT in the dark with a 1 mL 1:1 solution of glycerol:PBT (Sigma) followed by a 30 min incubation with a 1 mL 7:3 glycerol:PBT solution. Following this step, the glycerol solution was aspirated and replaced with 1 mL Mowiol mounting medium (Sigma). Using microscope slides, the aggregates were mounted using a cut P20 tip by pipetting a 17 µL droplet onto the slide. Then, using spacers attached to the slide to prevent the crushing of the aggregates, the coverslips were placed on top of the spacers. The aggregates should be then left for at least 12 h to settle on the slide at 4ºC before going into confocal imaging.

Image processing and statistical analysis

After confocal imaging and fluorescence microscopy, the images were measured, scaled and analyzed using Fiji© software. In confocal imaging, the images were acquired and quickly processed in Zen© software and, in the event of acquiring Z-stacks, they were then reconstructed and analyzed using Imaris© software.
The results were presented as mean ± standard error of the mean (SEM), displayed as the error bars. The significance of variability between results from various groups was determined by t-test when comparing datasets two at a time and by One-way ANOVA test when comparing more than two data sets, using GraphPad Prism software. The results were considered statically different when $p<0.05$. The associated subtitles are * for $p< 0.05$, ** for $p<0.005$ and *** for $p<0.001$ and **** for $p<0.0001$.

Results and Discussion

As mentioned above, the aim of this work was to optimize NMP generation through a 3D culture of gastruloids. In that sense, a protocol by Baillie-Johnson *et al* [14] was used as a basis for this work's optimizations (as summarized in Figure 1). Regarding that protocol, cells were seeded in a 96-well plate under low adhesion conditions and began to aggregate spontaneously through self-organization in suspension. Even if some aggregation was already visible after 24 hours in culture, it was after 48 hours that a chemical pulse was applied to activate Wnt agonists and promoted aggregate elongation. Afterwards, medium was changed daily as elongating gastruloids were observed and finally collected after 5 days in culture, when the protocol ended.
This work had only one significant difference to Baillie-Johnson's protocol, which was the culture of cells in presence of PLGA fibers from day 0 in culture. The remaining steps were the same for both protocols and a control group was provided by mESC culture without the addition of PLGA fibers to the medium.

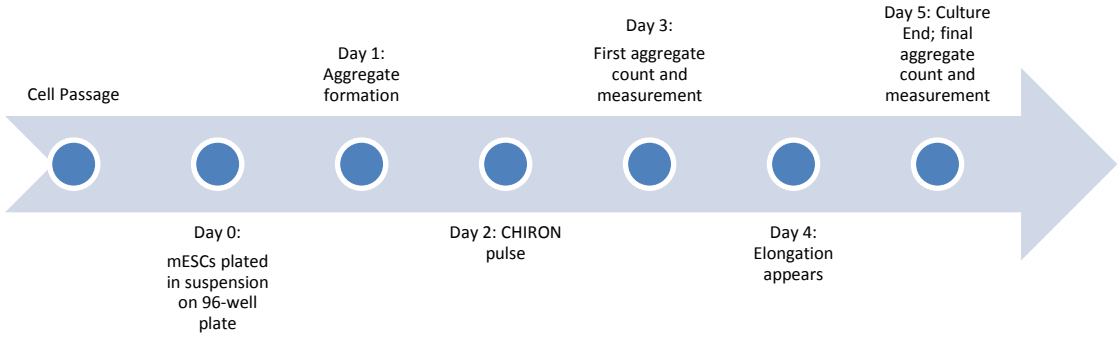

Figure 1: Summary of the protocol on which this work was based [14].

Afterwards, several approaches were used for measuring the obtained results: a morphological evaluation, based on the number of aggregates formed and elongates, as well as their maximum length; fluorescence detection studies for reporter cell lines to detect expression patterns for neural marker *Sox1* and immunofluorescence tests with relevant fluorescence markers were also performed. For the morphological analysis, two time points were chosen: at day 3 in culture, when aggregates achieve their biggest size before elongation was noticeable and after 5 days in culture, when the protocol ended (Figure 1).

PLGA fibers reduce variability in aggregate formation and elongation

Concerning the number of generated aggregates, at day 3, the efficiency was already very high when culturing mESCs without fibers. 88% of aggregate formation was reported on average in the control group, with a maximum of one counted aggregate per well. However, when PLGA was used, on average there was 99% of aggregate formation, with a maximum of one counted aggregate per fiber per well (Figure 2 A), which represents a statistically significant increase in aggregates formed when PLGA was used ($p<0.05$). Moreover, after 5 days in culture, the difference between groups was much more noticeable. Results reveal that on average, 78% of aggregates presented elongation when cultured in the presence of PLGA fibers, as opposed to 55% of elongated aggregates in control conditions. Nonetheless, standard conditions represented by the control group still provided robust results, with more than half of the wells on each 96-well plate on average containing elongated aggregates as expected. However, in the presence of PLGA fibers, aggregate elongation seems to be more efficient, reporting a statistically significant increase in the number of elongated aggregates by the end of the protocol ($p<0.001$).

PLGA fibers do not restrict aggregate length when present in culture

Regarding aggregate length, the question was raised if the use of PLGA fibers could lead to a negative effect on average gastruloid length, due to constrictions in cell-to-cell interaction imposed by a physical scaffold.
At day 3 in culture, the average measurement for aggregate size when cultured in the presence of PLGA fibers was 208 µm, while for the control group was 243 µm (Figure 2 B). This data shows that there is a statistically significant decrease in length when using PLGA fibers ($p<0.05$). Such a difference could be due to the fact that initially agglomerated cells in contact with the fiber may have had more restricted interactions with neighboring cells. On its turn, these constrictions could lead to a lower number of cells present initially when compared to control conditions, where cell movement is unrestricted). However, after 5 days in culture, the average length for PLGA aggregates was 498 µm versus 494 µm measured in the control group. Therefore, when the protocol ends, the average length in elongated PLGA aggregates was statistically similar ($p=0.55$) to the length in the control group, which suggests that the use of PLGA fibers does not have a negative effect on the elongation of the aggregates.

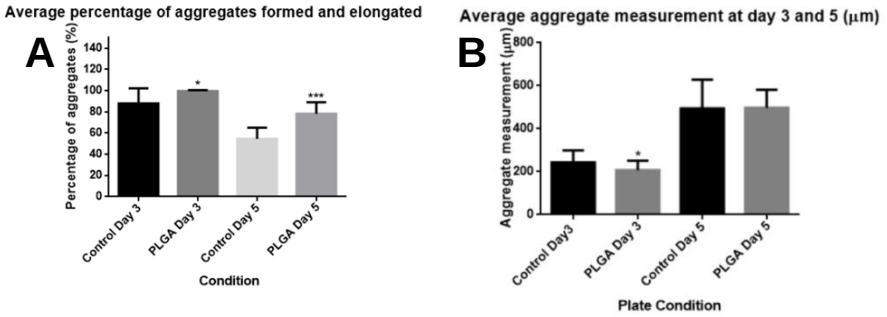

Figure 2: Average percentage (A) and length in μm (B) of aggregates formed at day 3 and elongated by day 5 in culture, with or without PLGA fibers, with standard deviation error bars. N=1152 experiments. *p<0.05; ***p<0.001

Aggregates present an organized Sox1 fluorescence pattern when cultured in the presence of PLGA fibers

Studies [24] show that the activation of the Wnt signaling pathway *in vitro* between 48-72h of the protocol results in the expression of *Sox1* only in the tip of the elongated gastruloid, as opposed to occupying its entire volume as when no Wnt activation is present and only anterior neural differentiation occurs.

Through the use of a reporter cell line *Sox1::GFP*$^{+}$, it was possible to determine the region of *Sox1* expression through fluorescence detection and to count the number of aggregates exhibiting the expected fluorescence pattern at the tip of the gastruloid.

The collected data showed that, on average, 75% of elongated PLGA aggregates displayed fluorescence in some of their volume, while 54% of the elongated aggregates in the control group also reported fluorescence in some part of the gastruloid's body. Confronting this data against the one collected from counting the elongated aggregates previously, it is possible to notice that almost every elongated aggregate displays some *Sox1*-related fluorescence, patterned or not.

However, not all of these aggregates showed the predicted pattern at the tip of the gastruloid. When searching for this pattern, it was observed that, on average, there are 66% of elongated PLGA aggregates on average exhibiting the expected fluorescent area versus 33% control aggregates (Figure 3). These results represent therefore a statistically significant increase ($p<0.0001$) in the number of aggregates demonstrating the expected area of fluorescence when cultured in the presence of PLGA fibers. Empirically, it was also possible to observe differences between the two datasets, since culture in the presence of PLGA fibers presented a highly patterned fluorescence area at the tip of the gastruloid, while in the absence of fibers the expression zones vary from the predicted ones to only covering a small portion of the tip or to covering the almost entirety of the aggregate (Figure 3).

Elongated aggregates display a region of neural tissue emerging alongside the PLGA fiber

Immunofluorescence tests were done in elongated aggregates after 5 days in culture, using *Sox2* and *Brachyury* (Bra) as NMP markers, to ask if the *Sox1::GFP* neural progenitors present in aggregate's tips were indeed NMPs. Results showed that in the tip of PLGA aggregates as well as in the control group there were regions with co-expression of both markers, indicating the presence of NMP populations in the extended gastruloids. This suggests that the use of PLGA fibers does not compromise NMP generation at regions predicted by the Literature (Figure 4 A; E) [14, 24].

These empirical observations were confirmed through analysis of histograms measuring pixel intensity for both markers. The analysis showed that histograms (Figure 4 F) had similar shapes for *Sox2* and *Bra* in each position of the region of interest, and intensity was within 20-80% for pixels in the images, therefore being attributable to real signal and not background noise (which would be beyond 20%) or pixel saturation (which would be closer to 100%), thus confirming co-expression of molecular markers used to characterize NMPs [24].

However, analysis of Sox2 expression in the PLGA aggregates revealed that, besides the characterization of NMP populations, it was possible to identify a region only *Sox2*$^{+}$ with little or no *Bra*$^{+}$ cells, emerging from extended aggregates cultured in the presence of PLGA fibers (Figure 4 B-D). This structure was not found in aggregates cultured without the polymer (Figure 5 E). Regarding its location, the tubular structure was observed alongside the polymer, following the same path described by the fiber.

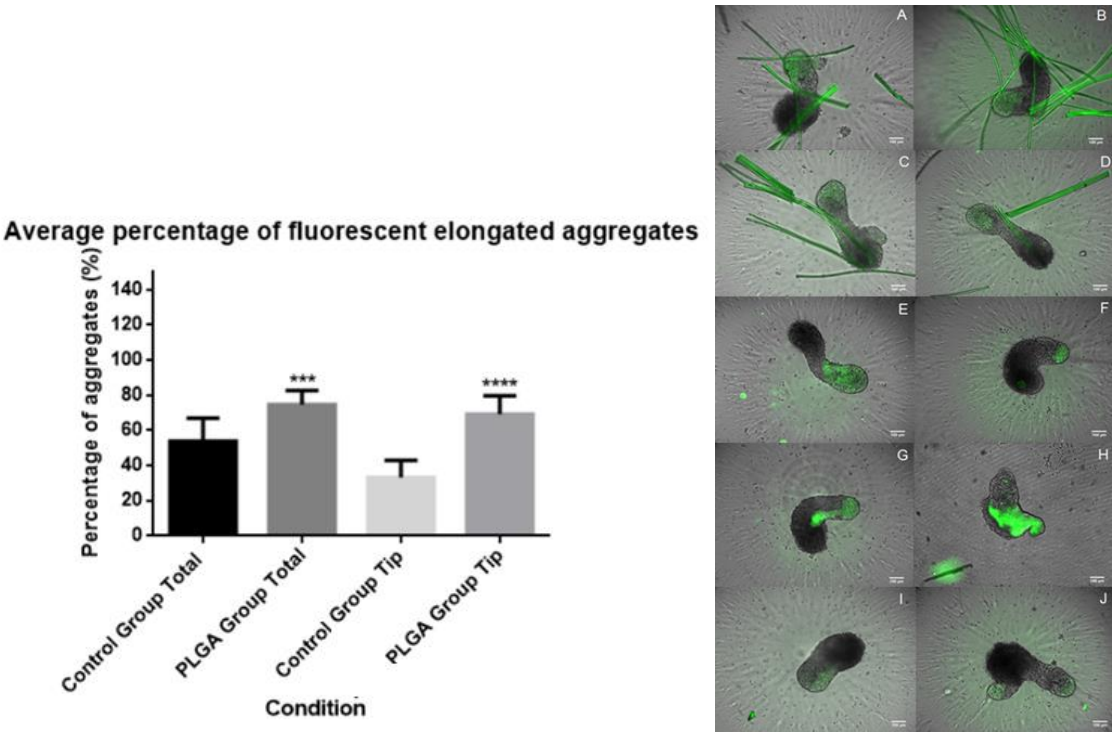

Figure 3: (Left) Quantification of the percentage of elongated aggregates with scattered Sox1::GFP$^+$ cells versus elongated aggregates with localized Sox1::GFP$^+$ cells at the elongating tip. N= 789 experiments. (Right) Aggregates at day 5 displaying Sox1::GFP fluorescence when cultured in presence of PLGA fibers (A-D), displaying a patterned fluorescent area at the tip of the gastruloid or in their absence (E-J), exhibiting a disorganized fluorescent area.

In control groups, no such structure was seen, with a population of *Sox2*$^+$-only cells also preceding the NMP region, but showing a scattered distribution and none of the organization that was present with PLGA fibers (See Figure 4 E).

This observation suggests that the use of PLGA fibers allowed the cells in the gastruloid near the polymer to respond to its mechanical stimulus and to develop neural tissue showing a structure resembling primordial neural tube, using the fiber as a reference for its organization.

Aggregates in presence of PLGA fibers display apicobasal epithelial polarization

After discovering the neural tube-like structure in the presence of PLGA fibers, it was important to assess if this structure was only the product of disorganized differentiation, using the polymer as a reference point, or if there was actually evidence of tissue organization.

In that sense, a different staining pattern was used to mark the PLGA aggregates, where *Bra* was replaced by *Zonula occludens-1* (*ZO-1)*, which has an expression related to membrane proteins typical of tight junctions and characteristic of apicobasal polarization in neural epithelial tissue [25, 26]. This pattern is present in the apical domain of the neural tube during its lumen development and it may be seen in neural rosettes *in vitro* during monolayer culture, for example [26].

Following 3D reconstruction of stained PLGA aggregates, it was possible to see the presence of highly stained regions for *ZO-1,* but also some occasional red spots expressing *ZO-1* outside of this region of interest and throughout the aggregate's body. However, this signal was most likely due to background noise or to saturated pixels associated with 'bright spots' during slice stacking by the software. This can be concluded from their bright intensity and disperse nature throughout the aggregate's body, not typical of true signal (Figure 5 A).

When zooming in on the region of interest (Figure 5 B-C), an organized expression of *ZO-1* was noticeable, in the 'honeycomb' pattern that is typical of apical polarization. This pattern was accompanied by expression of *Sox2* by the cells enveloped by *ZO-1*$^+$ cells. These observations suggest that in regions close to the PLGA fiber, the emergence of *Sox2*$^+$ populations arranged in a tubular shape also present patterns resembling apicobasal epithelial polarization, which hints that the use of the polymer allows the development of emergent neural tissue that presents evidence of tissue organization.

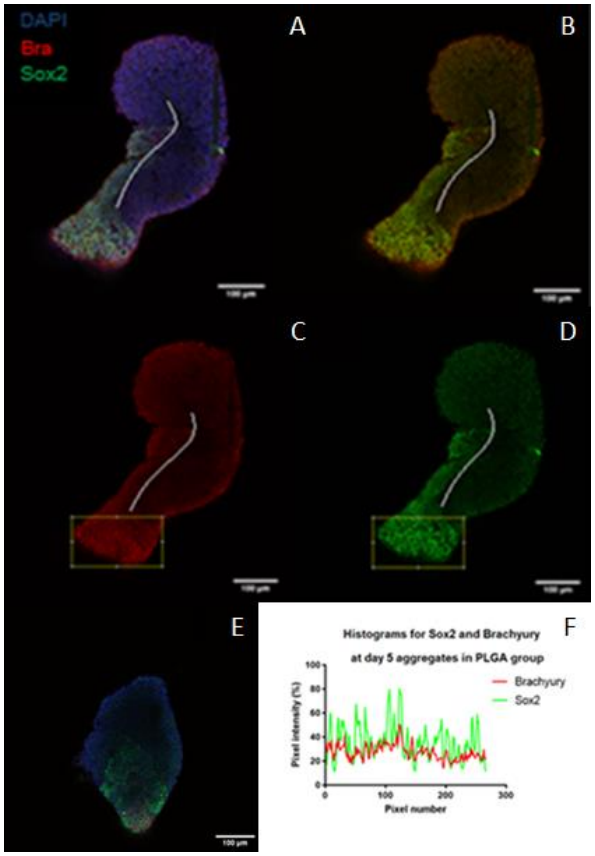

Figure 4: (A) Immunofluorescence of day 5 aggregate with Sox2 (Green), Bra (Red) and counterstained with DAPI (blue) as a control. NMP population at the tip of the aggregate is empirically visible (B), while also being evident the neural extension next to the PLGA fiber (marked in white) with an absence of mesodermal staining (C-D).In the absence of the PLGA fiber, while some $Sox2^{+}$ regions exist, they show a scattered distribution that lacks organization (E). (F) The presence of NMPs is confirmed by histogram analysis, in which both markers have the same profile shape for all locations inside region of interest (marked by yellow box).

Conclusions and future perspectives

The use of PLGA fibers in culture with mESCs aimed at optimizing the already existing protocol in which this work was based, by Baillie-Johnson *et al.* [14] to allow a more reproducible way to generate NMPs and achieve 3D gastruloids *in vitro* that would mimic *in vivo* gastrulation.

Morphological evaluation alone shows that the use of PLGA fibers increased the number of formed aggregates and, more importantly, of elongated aggregates in a substantial manner versus culture without the polymer, without changes in morphology or elongation length of gastruloids that could cause concern. The similarities in size of the aggregates for both groups may be related to chemical cues that prevent over-elongation after a certain point, much like in the mouse embryo *in vivo*, due to the role of Retinoic Acid (RA), whose activation marks the end of axial elongation in the embryo once gastrulation is complete. Thus, these are causes independent of the use of PLGA as a scaffold and related to the gastruloid's own microenvironment.

Furthermore, aggregates cultured together with the fibers also show a more organized *Sox1* expression pattern in the tip of the aggregates versus disorganized fluorescent areas in gastruloids cultured alone. They demonstrated variable fluorescent patterns that may either be the expected ones or be present throughout the aggregate's entire volume.

Regarding NMP generation, immunofluorescence tests also allowed detection of NMP populations that co-expressed *Sox2* and *Bra* at the tip of both PLGA aggregates and in the control group. These results showed that cell culture in the presence of the polymer did not compromise NMP generation.

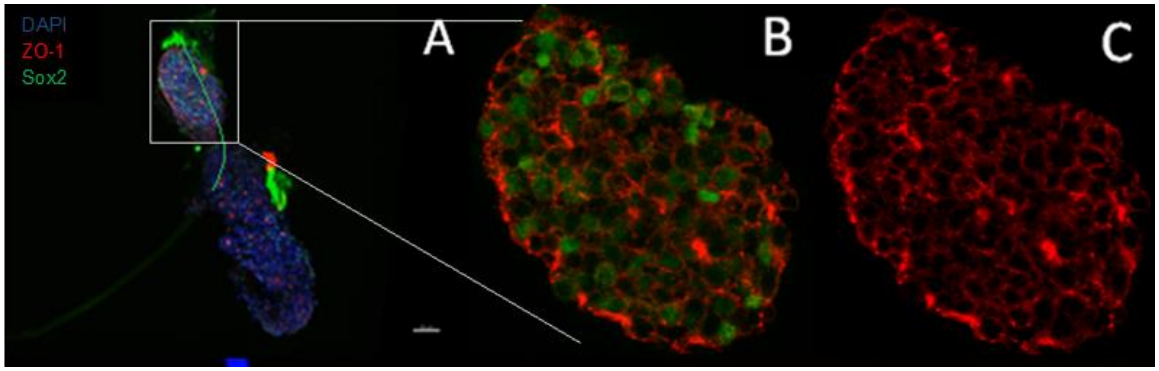

Figure 5: Day 5 aggregate cultured in the presence of PLGA fiber (marked in green) (A) stained for Sox2 (green) and ZO-1 (Red) and counterstained with DAPI (blue), showing Sox2 expression in cells enveloped by ZO-1 stained membranes, visible on a close-up (B-C). This staining pattern is associated with neural epithelial polarization as it is a hallmark of neural tube development.

These results suggest that the use of PLGA fibers does provide a more robust protocol allowing not only the generation of a higher number of gastruloids but also in a patterned manner and with no compromise towards tissue development.

While optimization of the protocol was the main goal of this work, the use of PLGA fibers also led to the emergence of neural tissue in regions close to the polymer. Besides its tubular shape, this neural population was characterized by *Sox2* and *ZO-1* expression, a pattern associated with neural epithelial polarization and characteristic of neural tube development.

This finding suggests the importance of the fiber in providing structural support and mechanical stimuli that other than promoting the elongation of the gastruloid, would simultaneously aid in neural differentiation, playing the role that the notochord plays *in vivo*. It is already well known that in embryonic development the essential stimuli are not only restricted to chemical ones [22, 23]. This work only highlights that tissue development and organization is a combined effort between chemical, physical and mechanical stimuli.

In the future, it would be interesting to see this combination further studied *in vitro.* Besides the use of a Wnt activator to cause elongation of the aggregate, cells could be cultured in the presence of fibers with a functionalized surface. This would allow dispersion of chemical stimuli associated with neural tube development, like Sonic Hedgehog, secreted by the notochord and responsible for neural tube development and closure. Another alternative could be the use of an embryonic notochord instead of a fiber to play its role as a signaling center. This would further answer some questions regarding the interplay between chemical and mechanical functions during neural development.

Future work in this direction could result in a protocol to efficiently generate 3D neural tube or, taking it a step further, even spinal cord, that would have endless applications in tissue engineering and disease modeling and could even open doors in translational approaches capable of improving spinal cord treatments based on cell therapies.

It would also be essential to test this protocol using other biomaterials (polymers or not) that would have different physical properties than PLGA, such as stiffness, hydrophobicity or surface patterning (through the use of techniques such as electrospinning to obtained differently shaped or sized fibers, for example). Comparative studies of this nature are essential towards providing a hypothesis on the cellular response in 3D when cultured in the presence of materials with different properties, and how those same properties would affect the efficiency of the aggregation and elongation processes *in vitro*. Overall this project was well succeeded in optimizing a previous protocol, combining cell culture with a bioengineering approach, hence resulting in the use of biomaterials in order to obtain a reproducible procedure with less variability. This project also accomplished to provide further insight into the importance of mechanical stimuli in tissue development and organization, frequently overlooked in favor of chemical and molecular responses. This was achieved through the development of neural tissue in contact with polymeric fibers that showed epithelial polarization indicating organized behavior, paving the way for possible novelties in 3D models for posterior central nervous system development *in vitro*.

Acknowledgments

I wish to thank Prof. Domingos Henrique (DHenrique Lab, IMM, Universidade de Lisboa) for accepting me as a Master's student and for all the advice that improved my work. I would also like to thank Prof. Margarida Diogo for her supervision and support throughout this project. I am also grateful to all members of DHenrique Lab for many interesting discussions. I would also like to acknowledge the technical facilities of IMM, namely the BioImaging group for providing their equipment and services. A final thank you to my family and friends for their support.

References

1. Tam, Patrick PL, and Richard R. Behringer. "Mouse gastrulation: the formation of a mammalian body plan." *Mechanisms of development* 68.1 (1997): 3-25.
2. Staveley, B. E. "Vertebrate Development I: Life Cycles and Experimental Techniques [WWW Document]." *Molecular & Developmental Biology* (2013).
3. Larsen, William James, and Lawrence S. Sherman. *Human embryology*. Vol. 1. New York: Churchill Livingstone, 1993.
4. Sadler, Thomas W. *Langman's medical embryology*. Lippincott Williams & Wilkins, 2011.
5. Rossant, Janet, and Patrick T. Tam. *Mouse development: patterning, morphogenesis, and organogenesis*. Gulf Professional Publishing, 2002.
6. Lowery, Laura Anne, and Hazel Sive. "Strategies of vertebrate neurulation and a re-evaluation of teleost neural tube formation." *Mechanisms of development*121.10 (2004): 1189-1197.
7. Copp, Andrew J., and Nicholas DE Greene. "Neural tube defects—disorders of neurulation and related embryonic processes." *Wiley Interdisciplinary Reviews: Developmental Biology* 2.2 (2013): 213-227.
8. Hans, J., et al. "Neurulation and neural tube defects." *Clinical Neuroembryology*. Springer Berlin Heidelberg, 2014. 165-217.
9. Copp, Andrew J., et al. "Spina bifida." *Nature Reviews Disease Primers* (2015): 15007.
10. Henrique, Domingos, et al. "Neuromesodermal progenitors and the making of the spinal cord." *Development* 142.17 (2015): 2864-2875.
11. Nieuwkoop, Pieter Dirk, and G. V. Nigtevecht. "Neural activation and transformation in explants of competent

ectoderm under the influence of fragments of anterior notochord in urodeles." *Development* 2.3 (1954): 175-193.

12. Nieuwkoop, P. D. "Activation and organization of the central nervous system in amphibians. Part III. Synthesis of a new working hypothesis." *Journal of Experimental Zoology* 120.1 (1952): 83-108.
13. Gouti, Mina, et al. "In vitro generation of neuromesodermal progenitors reveals distinct roles for wnt signalling in the specification of spinal cord and paraxial mesoderm identity." *PLoS Biol* 12.8 (2014): e1001937.
14. Baillie-Johnson, Peter, et al. "Generation of aggregates of mouse embryonic stem cells that show symmetry breaking, polarization and emergent collective behaviour in vitro." *Journal of visualized experiments: JoVE* 105 (2015).
15. Villanueva, Sandra, et al. "Posteriorization by FGF, Wnt, and retinoic acid is required for neural crest induction." *Developmental biology* 241.2 (2002): 289-301.
16. Logan, Catriona Y., and Roel Nusse. "The Wnt signaling pathway in development and disease." *Annu. Rev. Cell Dev. Biol.* 20 (2004): 781-810.
17. Clevers, Hans. "Wnt/β-catenin signaling in development and disease." *Cell*127.3 (2006): 469-480.
18. Fu, Jiang, et al. "Reciprocal regulation of Wnt and Gpr177/mouse Wntless is required for embryonic axis formation." *Proceedings of the National Academy of Sciences* 106.44 (2009): 18598-18603.
19. Gordon, Michael D., and Roel Nusse. "Wnt signaling: multiple pathways, multiple receptors, and multiple transcription factors." *Journal of Biological Chemistry* 281.32 (2006): 22429-22433.
20. Komiya, Yuko, and Raymond Habas. "Wnt signal transduction pathways."*Organogenesis* 4.2 (2008): 68-75.
21. Lancaster, Madeline A., et al. "Guided self-organization recapitulates tissue architecture in a bioengineered brain organoid model." *bioRxiv* (2016): 049346.
22. Levenberg, Shulamit, et al. "Differentiation of human embryonic stem cells on three-dimensional polymer scaffolds." *Proceedings of the National Academy of Sciences* 100.22 (2003): 12741-12746.
23. Guilak, Farshid, et al. "Control of stem cell fate by physical interactions with the extracellular matrix." *Cell stem cell* 5.1 (2009): 17-26.
24. Turner, David A., et al. "Wnt/β-catenin and FGF signalling direct the specification and maintenance of a neuromesodermal axial progenitor in ensembles of mouse embryonic stem cells." *Development* 141.22 (2014): 4243-4253.
25. Curchoe, Carol Lynn, Joseph Russo, and Alexey V. Terskikh. "hESC derived neuro-epithelial rosettes recapitulate early mammalian neurulation events; an in vitro model." *Stem cell research* 8.2 (2012): 239-246.
26. Abranches, Elsa, et al. "Neural differentiation of embryonic stem cells in vitro: a road map to neurogenesis in the embryo." *PloS one* 4.7 (2009): e6286.